Journal of Solar Energy Research (JSER)

Journal homepage: jser.ut.ac.ir

Photo-catalyst zinc ferrite-zinc oxide nanocomposites applicable for water purification under solar irradiation

Mahya Tamiji [a], Kambiz Hedayati[a,*], Davood Ghanbari[a]

[a]*Department of Science, Arak University of Technology, Arak 381814676, Iran*
Received: 2020-07-01
Accepted: 2020-10-10

Abstract

In this study, $ZnFe_2O_4$, ZnO nanoparticles and nanocomposites of $ZnFe_2O_4$–ZnO (core-shell) have been made via simple coprecipitation manner which is a rapid, inexpensive and economical method, impact of green surfactants such as red pepper, black pepper, lemon, saffron, as well as carbohydrates like gelatin, poly vinyl pyrrolidone, glucose, on morphology of $ZnFe_2O_4$ were investigated. These surfactants are known as biodegradable and biocompatible factors, moreover, the effect of concentration, temperature and sediment agent on the surface characteristics of core magnetic have been studied and outcomes of SEM analysis indicated that the organic solvent of the red pepper possesses a great effect on diminishing size of nanoparticles. Vibrating sample magnetometer (VSM) analysis emphasized that $ZnFe_2O_4$ and desired nanocomposites possess super-paramagnetic property and analysis such as X-ray diffraction and Fourier-transform infrared (FT-IR) spectroscopy were used to indicate pure nanoparticles and nanocomposites. As well photo-degradation of toxic dyes was applied under solar irradiation.

Keywords: Nanostructures; Photo-catalyst; solar irradiation; Zinc Ferrite; Zinc Oxide

Introduction

As we know, the various industries (textile, leather or dyeing and etc) generate colored effluent which are carcinogenic for humans and very harmful for the environment [1-2] .By the time pass various techniques have been utilized to eliminate these contaminants for instance, chemical, physical and biological procedures [3-5]. But nowadays, the advanced oxidation techniques has been considered greatly because of its low cost and potential features of this techniques, as well as its being fast [6-7]. Researches have proven that as the particle s shrink on nanoscale, the property of material also alters drastically, these properties such as physical, electrochemical, magnetic or even particle optical property [8-9]. Indeed amount of changes in these properties depends on the size of particles and their structure, approach of the preparation as well as temperature or time of preparing or their doping level [9-12]. For instance, at the bulk $ZnFe_2O_4$, zinc ions (Zn^{2+}) don't present any magnetic moment from themselves, but on nanoscale they exhibit very good magnetic properties [13-15]. And also, this material is considered as one of the candidates for photocatalytic degradation because of its high frequency and low toxicity and high sensitivity to

*k-hedayati@arakut.ac.ir

sunlight [16-17]. However many flaws of these nanomaterials and high electron and hole coupling have led to decrease the photocatalytic activity of these substances [18-20]. On the other hand, ZnO semiconductor (with broad band gap of 3.0–3.5 eV and exciton energy of 60 MeV) possesses high photocatalytic ability in ultraviolet radiation and underperforms in visible light [21-22]. Guo and his colleagues revealed during researches that $ZnFe_2O_4$ semiconductor (p-type) connection to ZnO semiconductor (n-type) leads to decline electron and hole coupling and to boost photocatalytic activity in the visible rang [23-25]. In this paper, by applying of coprecipitation procedure which is a fast chemical method at low temperatures. We combined ZnO (with shell role) and $ZnFe_2O_4$ (with magnetic core role), ultimately we prepared the $ZnFe_2O_4$ –ZnO nanocomposites with high photocatalytic potential and of course recyclable.

2. Experimental

2.1. Materials and methods

All of the chemical materials which used in this research have been manufactured by Sigma-Aldrich or Merck and were used without filtration, these materials with analytical grade include the following materials: $Zn(NO_3)_2$, $Fe(NO_3)_3.9H_2O$, NaOH, glucose, , Poly vinyl pyrrolidone and Gelatin, black and red pepper extract as well as saffron and lemon. X-ray patterns of each crystal structure were recorded by using Phillips XRD device via radiation of CuKα as well as the average size of crystals was assessed via Scherrer formula, $D=0.9K/\beta Cos\theta$ that, D assigns average crystals size, λ is indicant X-ray wavelength in nanometers (for CuKα=0.154 nm), β is determinant peak width at moiety maximum in radian and θ is angle of diffraction in radian. To determine nanoparticles morphology and structure of crystals, SEM (LEO Instrument 1455VP). Destruction potential and photocatalytic property of particles were evaluated via UV-Visible device (Thermo Helios Omega). Magnetometer device or VSM (Meghnatis kashan of company Iran) described magnetic behaviour of sedimentary nanoparticles with magnetic field 10k Oe at Room temperature and magnetic field 10 kOe. As well in this article, FT-IR device (Shimazu 470) was used to identify elements and their links.

2.2. Synthesis of $ZnFe_2O_4$ nanoparticles

In this study nanoparticles and nanocomposites were prepared via available coprecipitation approach at room temperature and the desired solvent in this method is deionized water also, we used NaOH (1M) to precipitate solution.

Initially 0.2 g of zinc nitrate($Zn(NO_3)_2$) and 0.85 g of iron nitrate ($Fe(NO_3)_3.9H_2O$) were mixed according to stoichiometry relationship in 200 ml of mention solvent, and after being dissolved by virtue of magnitude stirrer, added 10 ml of NaOH sediment agent to solution to reach pH=10. After mixing for 30 minutes, desired solution was washed with distilled water and centrifuged (for 3 minutes and 2000 rpm) and ultimately the achieved brown precipitate was dried at 80ºC (Fig.1).

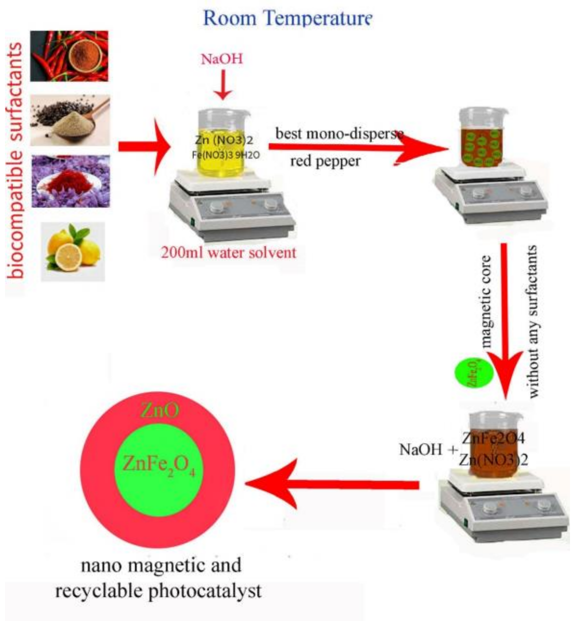

Figure 1. Schematic of provision nanocomposite $ZnFe_2O_4$-ZnO.

2.3. Synthesis of $ZnFe_2O_4$-ZnO

In this study, $ZnFe_2O_4$ –ZnO nanocomposites were synthesized with molar ratio of 50 to 50 percent, initially 1g of Sedimentary $ZnFe_2O_4$ was added to

100 ml of deionized water. In the next step, 0.5 g of $Zn(NO_3)_2$ was added to scattered ferrite in the solution and was allowed for one hour, the solution was mixed on a magnetic stirrer, after that, the required amount of sediment agent was added (5cc) to reach pH=10 and after half one hour, the desired solution was washed several times, and was denote by virtue of centrifuge and ultimately washed and dried at 80 ºC.

2.4. Photo-catalytic degradation process

The photocatalytic feature of the synthesized materials were measured via disintegration of azo dyes that these dyes are as models of organic contaminant, to carry out this work. Normally, 1 g of the desired catalyst was stirred in 10 ml of dye solution (in the dark for an hour), the necessity of this operation is to achieve the interaction of absorption through the samples. Then, after one hour, the solution was put under solar irradiation and sampling was performed every 5 min, and these samples were collected through centrifuge and their concentration changes were recorded via UV-Visible device.

3. Results & Discussion

Fig.2 affirms that the XRD pattern of synthesized samples of $ZnFe_2O_4$ conforms to the cubic phase pattern of pure zinc ferrite and Deby-Sherrer equation estimated average size of crystalline to be about 38 nm.

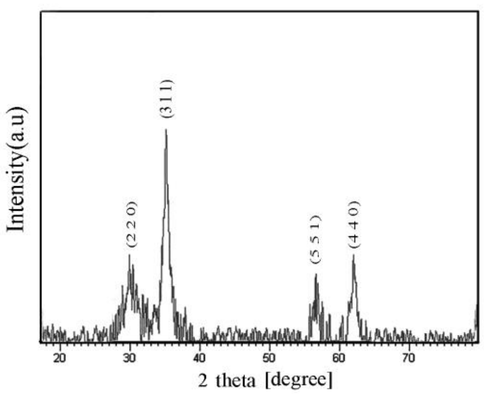

Figure 2. XRD pattern of $ZnFe_2O_4$ nanostructures

Fig.3 represents X-ray diffraction pattern of ZnO. This pattern reveals the formation of nanoparticles with a hexagonal phase (JCPDS No.:800075) and P63-mc space group that is correspondent with its pure zinc and the average size of crystals was computed 39 nm. The XRD pattern of $ZnFe_2O_4$-ZnO nanocomposite has been monitored in Fig.4. This pattern indicates the existence of cubic phase of pure zinc ferrite and hexagonal phase of pure zinc oxide. The average size of crystals for three peak with greater intensity was calculated 40 nm.

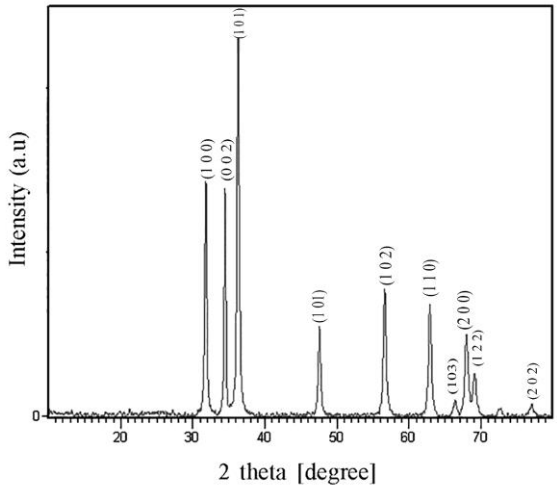

Figure 3. XRD pattern of ZnO nanostructures

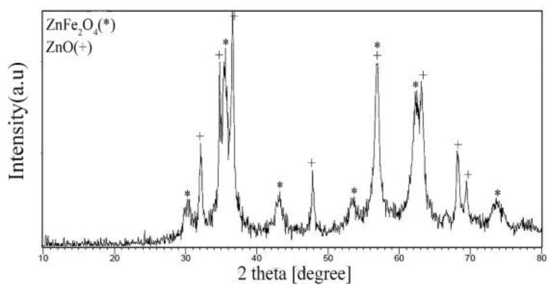

Figure 4. XRD pattern of $ZnFe_2O_4$-ZnO nanocomposite

Fig.5a indicates morphology of produced $ZnFe_2O_4$ nanoparticles by SEM device. The average diameter of these adhered nanoparticles is about 35 nm. These particles were synthesized without using any surfactants and in this study, this reaction was selected as the main and basic reaction. Next figure (Fig.5b) shows the impact of calcination temperature on particles size. Nanoparticles of zinc ferrite were calcined at 500 ºC for 2 hours. Indeed increasing calcination temperature led to trifle growth of particles, meanwhile mono-disperse nanoparticles were acquired as an amazing result.

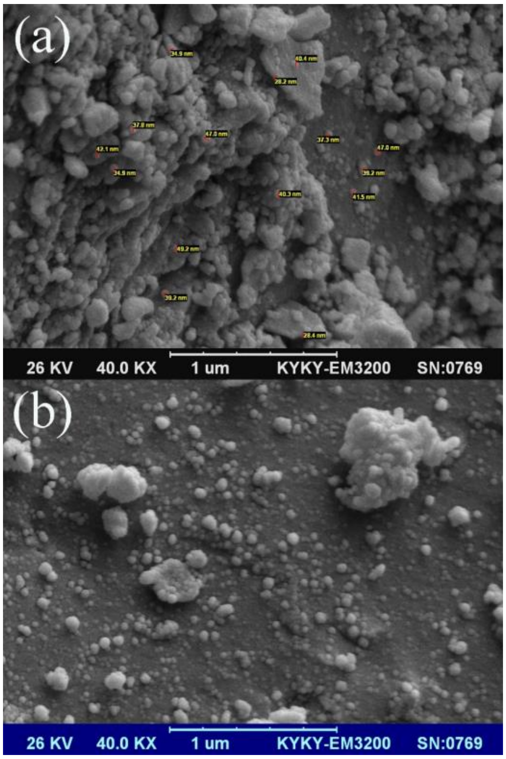

Figure 5. SEM images of zince ferrite (a) without using any surfactant (b) higher calcination temperature

In order to observe the influence of change in concentration on the shape and size of particles, we diluted the solution by increasing the solvent volume (100 to 200 ml). The results represent that similar nanoparticles with average size of 50 nm have been prepared (Fig.6). Fig.7 a, b indicates nanoparticles morphology by using surfactant poly vinyl pyrrolidone and as we observe zinc ferrite of nanoparticles adhere each other in the presence of this capping agent and tend to grow more (less than 80 nm). Existence of glucose green agent provides particles with almost spherical morphology and agglomeration with average size of about 50 nm (Fig.7 c, d.).

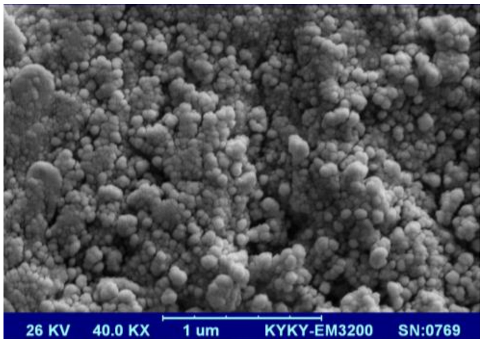

Figure 6. SEM image of zinc ferrite by decreasing concentration

Fig.8 a, b. illustrates the impact of Gelatin on morphology of particles, it's obvious that using of this surfactant leads that growth process overcome on nucleation, and we come across more agglomerated particles (average size of about 45 nm). We find out from Fig.8 c, d that raising temperature during the synthesis of zinc ferrite of nanoparticles diminishes the opportunity of nucleation of nanoparticles and produces pretty large nanoparticles (about 50 nm).

To test and evaluate the green synthesis of product, some fruits and vegetables were utilized as a new sort of biocompatible surface active factor Fig.9 a-c indicates products in the presence of black pepper extract, and SEM images represent the formation of regular spherical nanoparticles and mono disperse (average diameter 45). Saffron as another capping factor was employed and images prove generation of agglomerated nanostructures with average dimension about less than 100 nm (Fig.9 d). Outcomes of Fig 10. a, b show that spherical nanoparticles were prepared with average diameter around 60 nm by using lemon extract. Red pepper was also added to the solution and images show synthesis of nanoparticles with average size about 37 nm. Results approve the best mono-disperse and smallest particles were achieved in the presence of red pepper (Fig.10 c, d).

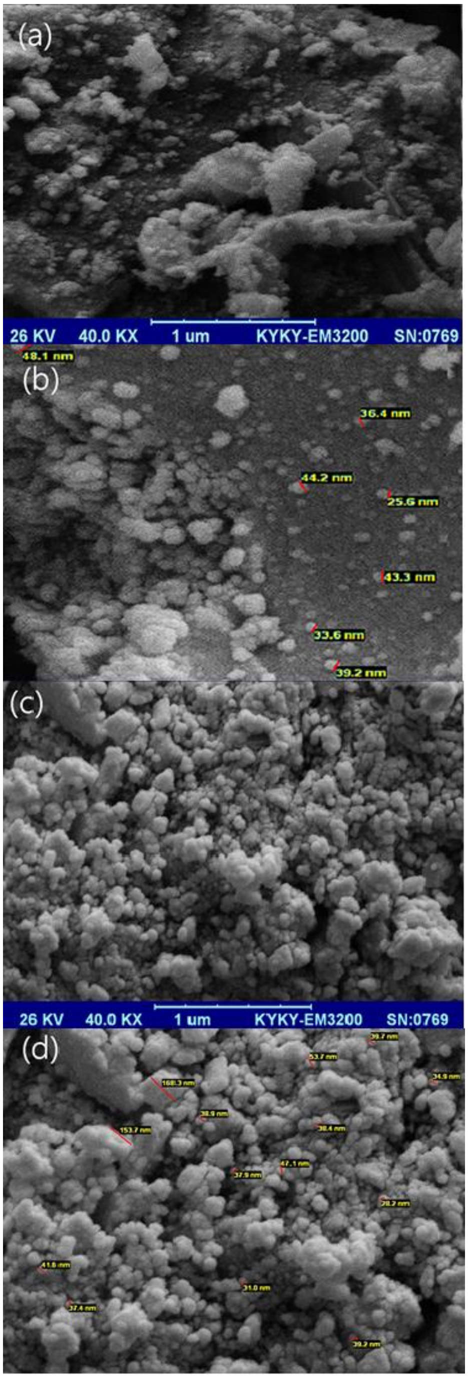

Figure7. SEM images of zinc ferrite nanoparticles(a,b) PVP (c,d) glucose

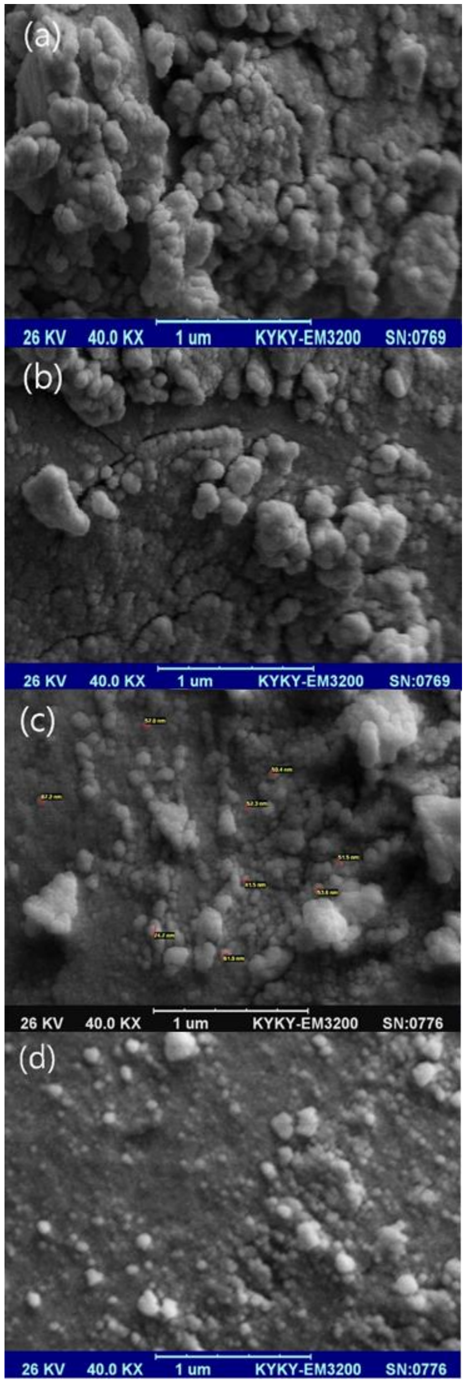

Figure 8. SEM images of zinc ferrite (a,b) by gelatine(c,d) temperature 150 ºC

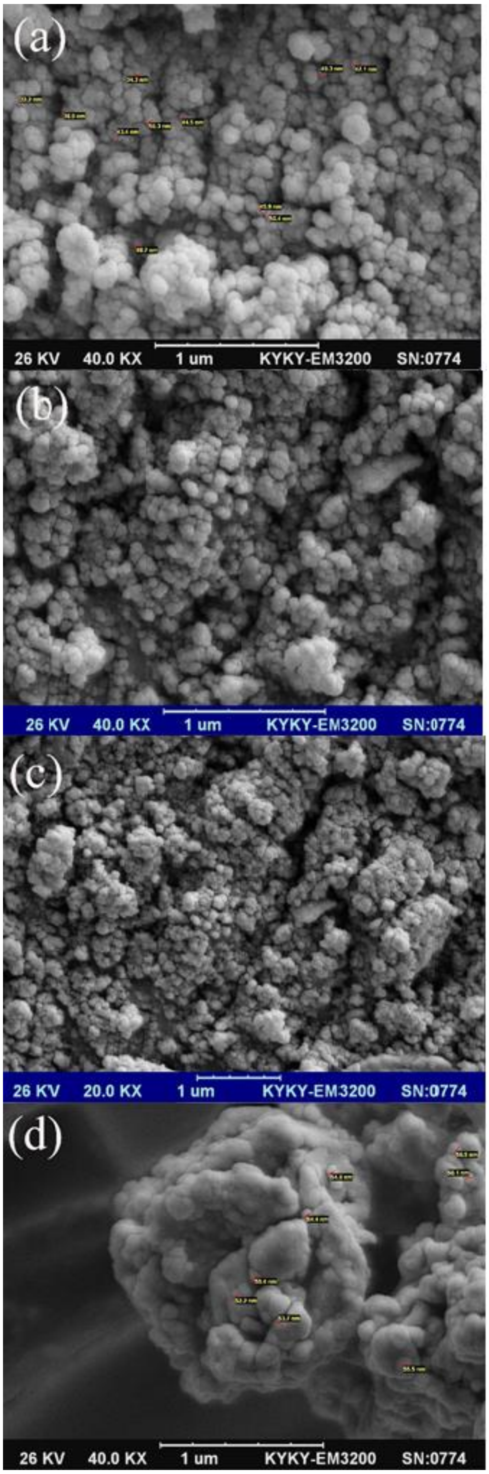

Figure 9. SEM images of zinc ferrite in the presence of (a, b, c) black pepper (d) saffron

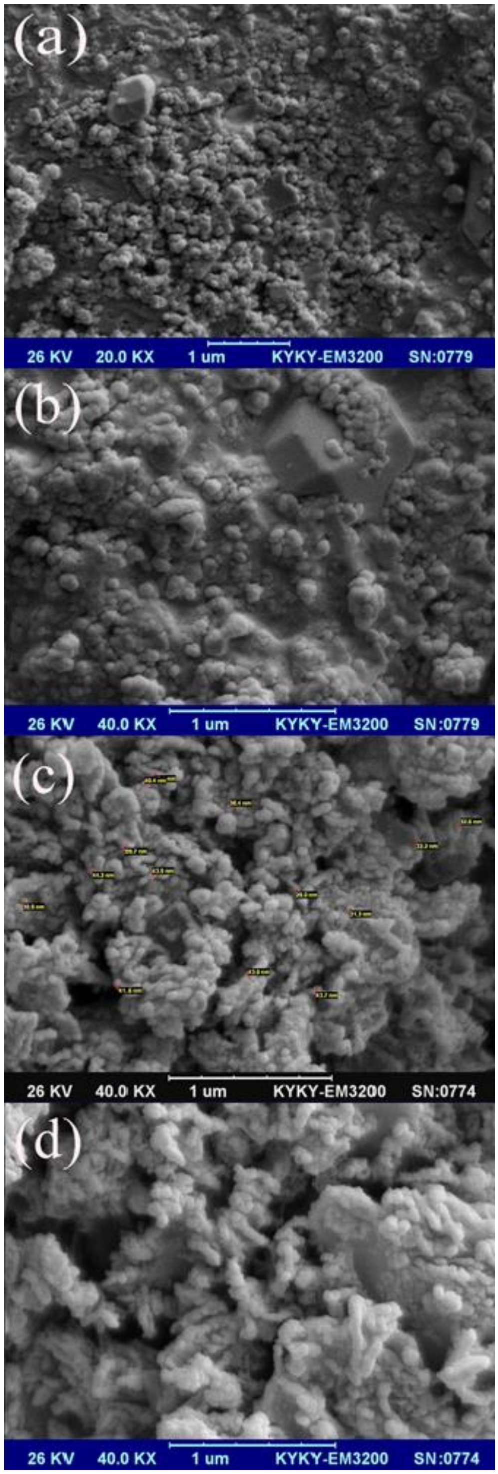

Figure 10. SEM images of zinc ferrite in the presence of (a, b) lemon (c, d) red pepper

Fig.11 a, b displays SEM images of synthesized nanoparticles of zinc ferrite via hydrothermal procedure (at 180 ºC for 5 h). Size of these nanoparticles is larger than, it's coprecipitation state (about 45 nm). In the second part of this figure (Fig.11c) coprecipitation synthesis of zinc oxide has been indicated. These particles possess average diameter of about 40 nm. Fig.12 shows SEM images of produced nanostructure of ZnO via hydrothermal procedure (at 180 ºC for 5 h) with average diameter size which is less than 43 nm.

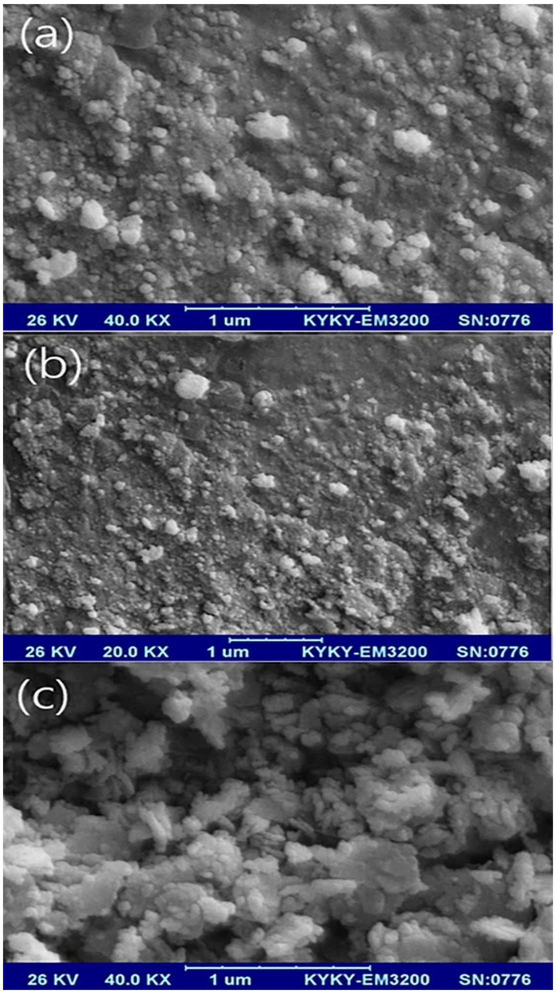

Figure11. SEM images (a,b) of zinc ferrite by hydrothermal method (c) ZnO nanoparticles

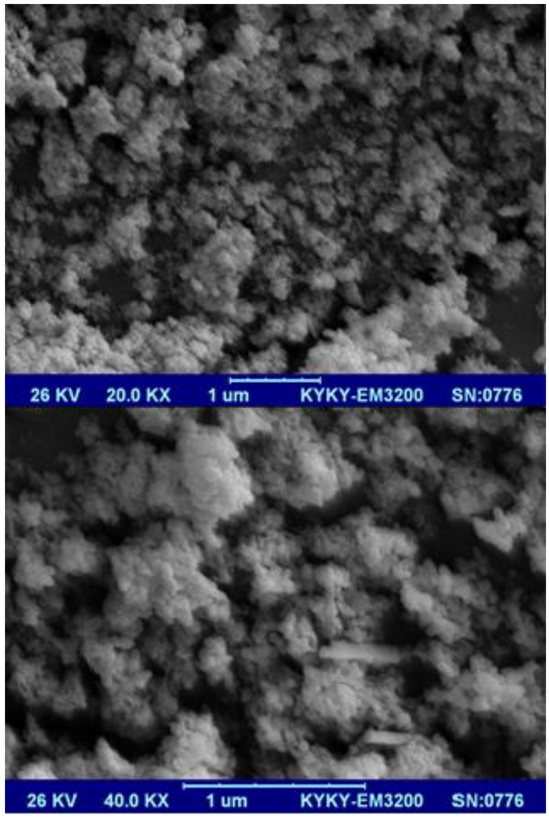

Figure 12. SEM images of ZnO hydrothermal nanoparticles

To make a magnetic and photocatalyst produce, a composite containing of both zinc ferrite and ZnO with 50:50% molar ratio was constructed. Figs.13 illustrates SEM images of the $ZnFe_2O_4$-ZnO nanocomposite that confirms amazing mono-disperse star-like nanocomposites were obtained which diameter of every single branch is around 45 nm.

FT-IR spectrum of precipitation nanoparticles of $ZnFe_2O_4$ by applying lemon extract is illustrated in Fig.14. Absorption peak at 500-600 cm-1 is representative Fe-O and Zn-O bonding as well as wide absorption peak at 3300-3400 cm^{-1} and weak peak at 1564 cm^{-1} are associated with O-H and H–O–H bonding respectively. Absorption peak of 1300-1400 cm^{-1} assigned to C=O bonds of the nitrate group of zinc precursor and the citric acid in the lemon extract.

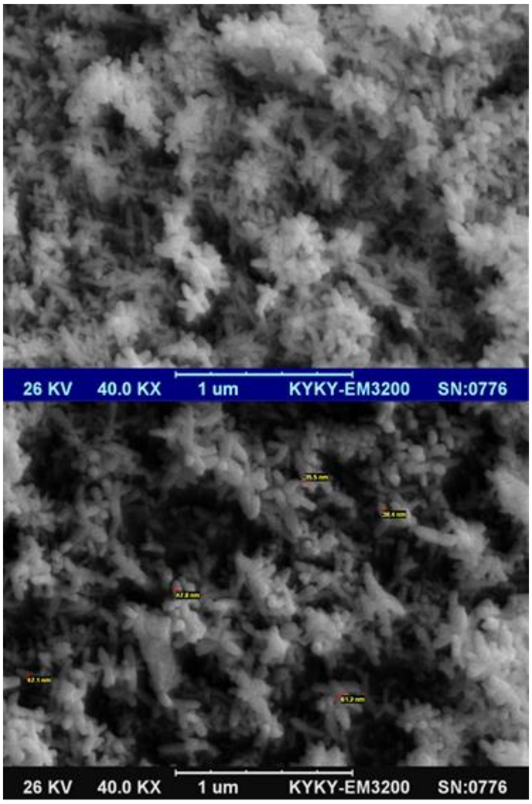

Figure 13. SEM images of $ZnFe_2O_4$-ZnO nanocomposite.

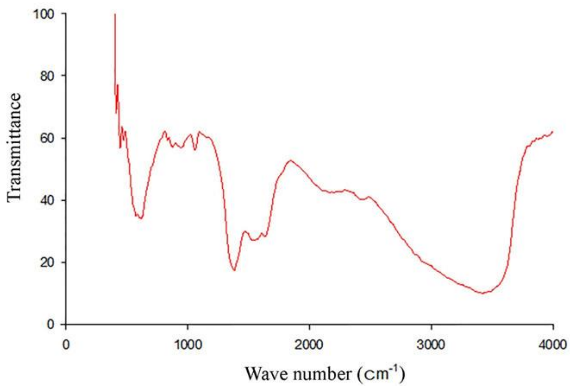

Figure 14. FT-IR spectrum of $ZnFe_2O_4$ nanoparticles

Fig.15 illustrates FT-IR spectrum of precipitation nanoparticles of ZnO, observed absorptions at 400-700 cm^{-1} are related to Zn-O bond and existence of wide peak at 3300-3400 cm^{-1} is associated with hydroxyl group.

Finally, Fig.16 confirms the formation of nanocomposites of $ZnFe_2O_4$-ZnO without impurities. Indeed, in this spectrum the bonding of magnetic nanoparticles is observed at sharp peak of 700-800 cm^{-1} (Zn-O and Fe-O bonds). Wide absorption at 3400-3600 cm−1 corresponds with O-H group. Absorption at 1300-1700 cm^{-1} is assigned with nitrate group of zinc precursor. C-O (at 900-1000 cm^{-1}) and C=O (at 1300-1700 cm^{-1}) bonds as well as C-H (at 2900-3000 cm^{-1}) of lemon extract are depicted in spectrum.

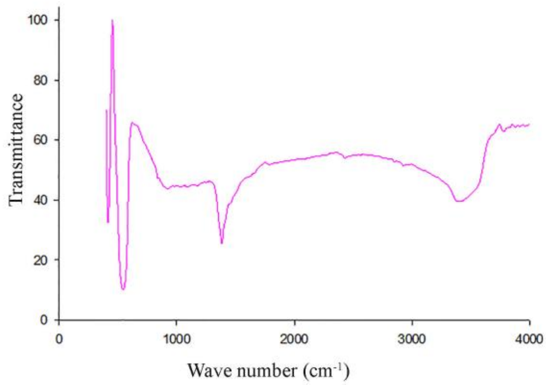

Figure 15. FT-IR spectrum of ZnO nanoparticles

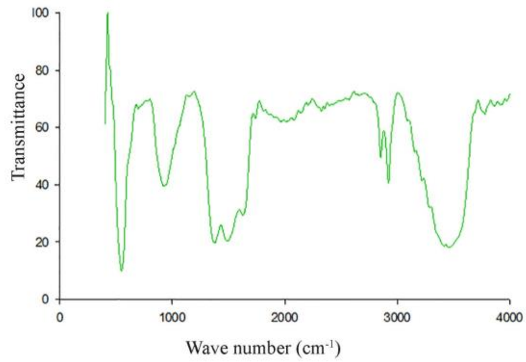

Figure 16. FT-IR of spectrum $ZnFe_2O_4$-ZnO nanocomposite

Fig.17 illustrates magnetic property of produced $ZnFe_2O_4$ (surfactant-free) at 25 ºC temperature. Outcomes of this curve represent super-paramagnetic behaviour of products with saturation magnetization about 16.17 emu/g and coercivity about Zero Oe. Fig.18 illustrates super-paramagnetic trait of $ZnFe_2O_4$ (in calcination temperature of 500 ºC), as well as indicates saturation magnetization about 16.39emu/g and coercivity of about zero Oe for these nanoparticles. As is illustrated in Fig.19, prepared nanocomposites of $ZnFe_2O_4$-ZnO indicate super-paramagnetic trait with saturation magnetization about 13.26 emu/g. and coercivity around Zero Oe.

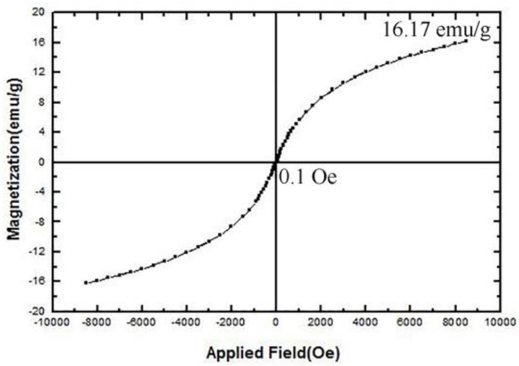

Figure17. VSM of zinc ferrite nanoparticles prepared at 25 ºC

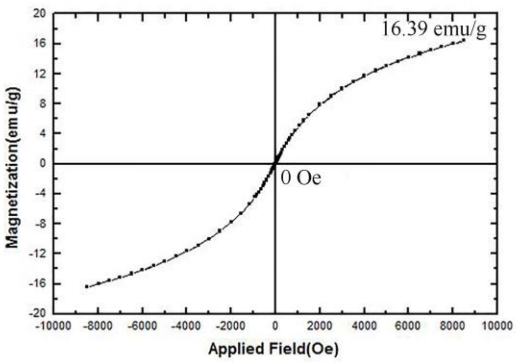

Figure 18. VSM of $ZnFe_2O_4$ nanocomposite synthesized at calcination temperature of 500 ºC

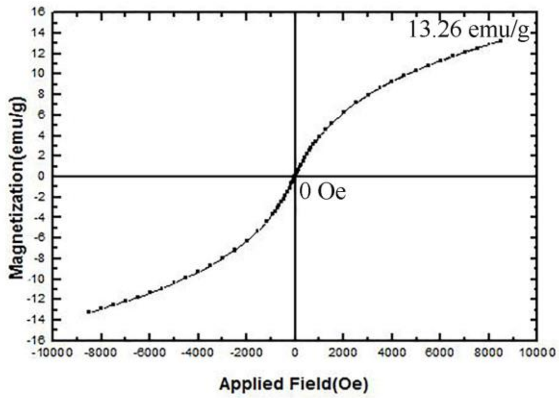

Figure 19. VSM of $ZnFe_2O_4$-ZnO- nanocomposite

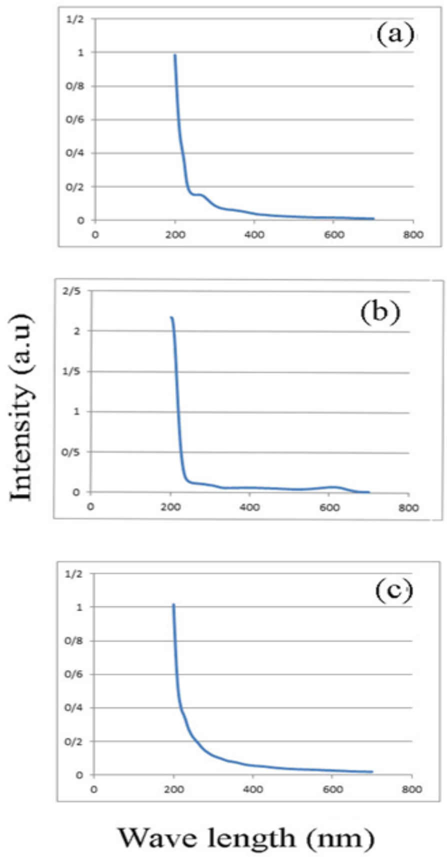

Figure 20. UV-Vis absorption in the presence of ZnO (a) acid violet (b) acid blue (c) acid black

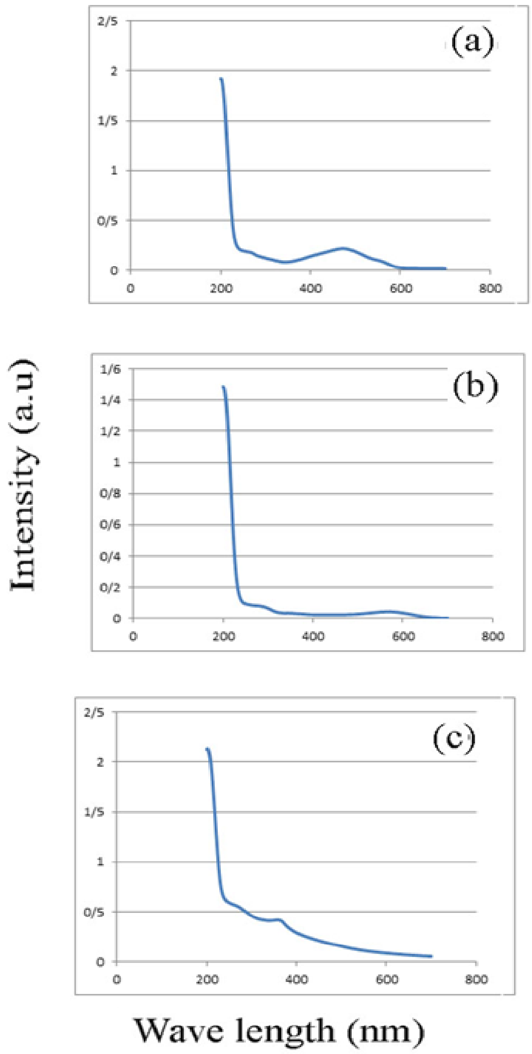

Figure 21. UV-Vis absorption in the presence of $ZnFe_2O_4$-ZnO (a) acid violet (b) acid blue (c) acid black

One of the advantages of magnetic behaviour of this nanocomposites is the easy removal of the reaction by magnet and its being renewable for photocatalytic applications.

UV-Vis absorption of photo-degradation of violet acid, blue acid and black acid are shown in Fig.20 a-c, in the presence of ZnO. Also UV-Vis absorption of violet acid, blue acid and black acid are illustrates in Fig.21 a-c in the presence of $ZnFe_2O_4$-ZnO prepared nanocomposites.

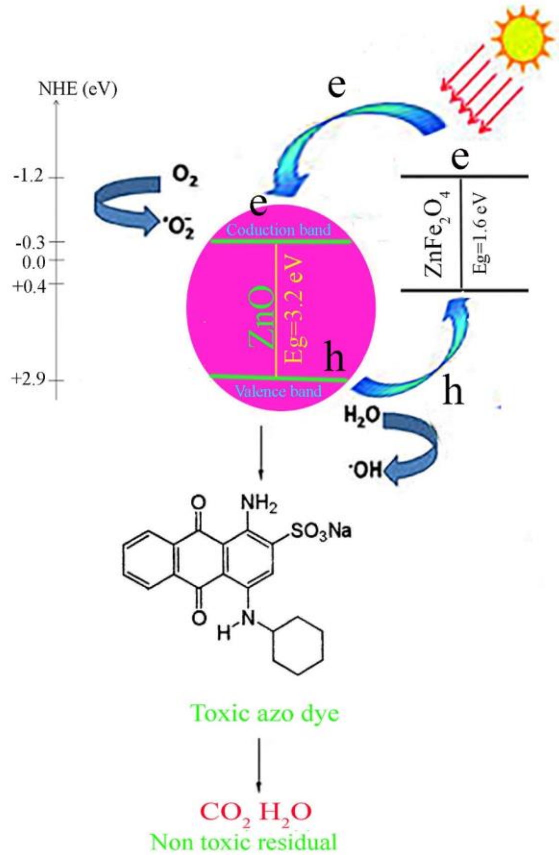

Figure 22. Photo-catalyst mechanism in degradation of toxic dyes

In this segment, violet acid, blue acid and black acid are utilized as an example of organic contaminant and that's due to their molecular structure and comparative firmness. λ_{max} of mention dyes were approved by scientific literature. The photocatalytic trait of formed $ZnFe_2O_4$-ZnO nanocomposites leads that these nanoparticles are utilized to eliminate toxic water contaminant and reduce environmental problems. Photo-degradation mechanism of $ZnFe_2O_4$-ZnO nanocomposite is indicated in Fig.22 schematically. The effect of solar light irradiation on changing the concentration of solution containing a catalyst is indicated in Fig.23. By the time pass and further decline concentration of azo dyes, the peak of absorption of these dyes reduces and evanesce around 15 min (for black acid),18 min (for violet acid) and 20min (for blue acid).

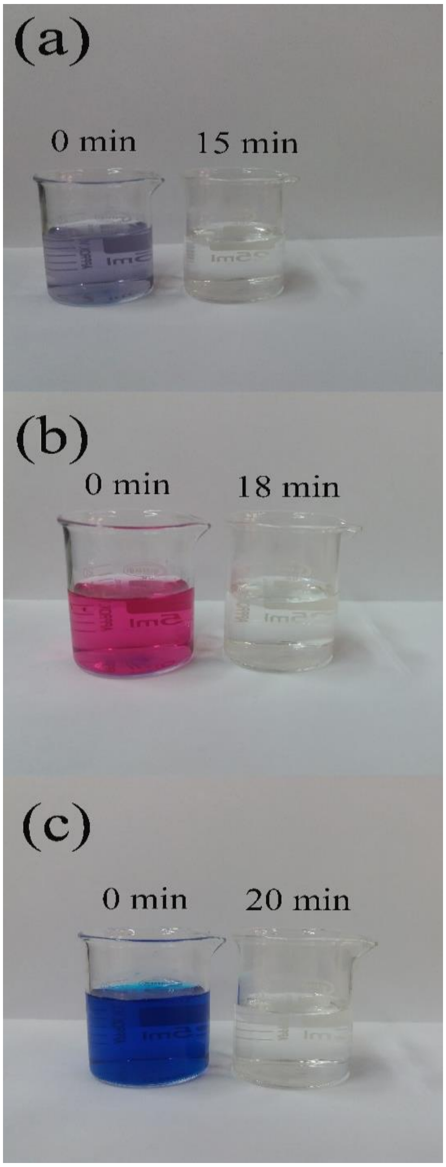

Figure 23. Photo-degradation of (a) acid black (b) acid violet (c) acid blue under solar light

4. Conclusions

New and biocompatible magnetic $ZnFe_2O_4$-ZnO nanocomposites were reported that can photo-degrade toxic azo dyes. SEM confirmed that by temperature and volume changes of solvents, agglomerated products with bigger sizes were prepared while by using red pepper extract the best mono-disperse nanoparticles were synthesized. VSM proved that prepared nanoparticles and nanocomposites present super-paramagnetic trait. Magnetic saturation was diminished due to existence of shell on core. The photocatalytic trait of $ZnFe_2O_4$-ZnO nanocomposite was monitored by degradation of three different azo dyes by using solar light. The outcomes demonstrate that coprecipitation approach is an easy and economical manner for synthesis of $ZnFe_2O_4$-ZnO nanocomposites and moreover the prepared nanocomposites are appropriate candidate for photocatalytic operation. The fastest degradation was for black acid in 15 min.

References

1. Shu, R., et al., *Facile design of nitrogen-doped reduced graphene oxide/zinc ferrite hybrid nanocomposites with excellent microwave absorption in the X-band*. Materials Letters, 2019, **255**: 126549.
2. Sobahi, T. R., and M. S. Amin, *Synthesis of ZnO/$ZnFe_2O_4$/ Pt nanoparticles heterojunction photocatalysts with superior photocatalytic activity*. Ceramics International, 2020, **46**: p. 3558-3564.
3. Su, J., et al., *Construction of heterojunction $ZnFe_2O_4$/ZnO/Ag by using ZnO and Ag nanoparticles to modify ZnFe2O4 and its photocatalytic properties under visible light*. Materials Chemistry and Physics, 2018, **219**: p. 22-29.
4. Rabbani, M., et al. *Synthesis of TCPP/$ZnFe_2O_4$@ ZnO nanohollow sphere composite for degradation of methylene blue and 4-nitrophenol under visible light*. Materials Chemistry and Physics, 2016, **179**: p. 35-41.
5. Chandel, N. at al., *Magnetically separable ZnO/$ZnFe_2O_4$ and ZnO/$CoFe_2O_4$ photocatalysts supported onto nitrogen doped graphene for photocatalytic degradation of toxic dyes*. Arabian Journal of Chemistry, 2020,**13**: p. 4324-4340.

6. Ahmad pour, N., et al., *A potential natural solar light active photocatalyst using magnetic $ZnFe_2O_4$ @ TiO_2/Cu nanocomposite as a high performance and recyclable platform for degradation of naproxen from aqueous solution*. Cleaner Production, 2020, **268**: 122023.
7. Keterew Kefeni, K., and B. *Brilliance Mamba, Photocatalytic application of spinel ferrite nanoparticlesand nanocomposites in wastewater treatment: Review.* Sustainable Materials and Technologies, 2020, **23**: e00140.
8. Baynosa, M. L., et al., *Eco-friendly synthesis of recyclable mesoporous zinc ferrite@ reduced graphene oxide nanocomposite for efficient photocatalytic dye degradation under solar radiation.* Colloid and Interface Science, 2020, **561**: p. 459-469.
9. Bayat, R., et al., *A magnetic $ZnFe_2O_4$/ZnO/perlite nanocomposite for photocatalytic degradation of organic pollutants under LED visible light irradiation*. Solid State Sciences, 2019, **89**: p. 167-171
10. Falak, P., et al., *Synthesis, characterization, and magnetic properties of ZnO-$ZnFe_2O_4$ nanoparticles with high photocatalytic activity*. Journal of Magnetism and Magnetic Materials, 2017, **441**: p. 98-104.
11. Choodamani, C., *Structural, electrical, and magnetic properties of Zn substituted magnesium ferrite*. Ceramics International, 2016, **42**: p. 10565-10571.
12. Hedayati, K., *Fabrication and Optical Characterization of Zinc Oxide Nanoparticles Prepared via a Simple Sol-gel Method*. Journal of Nanostructure, 2015, **5**: p. 13-16.
13. Joulaei, M., et al., *Investigation of magnetic, mechanical and flame retardant properties of polymeric nanocomposites: Green synthesis of $MgFe_2O_4$ by lime and orange extracts*. Composites Part B: Engineering, 2019 **176**: 107345.
14. Nabiyouni, G., and D. Ghanbari, *Simple preparation of magnetic, antibacterial and photo-catalyst $NiFe_2O_4$@TiO_2/Pt nanocomposites*. Journal of Nanostructures, 2018, **8**: p. 408-416.
15. Kiani, A., et al., *A novel magnetic $MgFe_2O_4$–$MgTiO_3$ perovskite nanocomposite: Rapid photo-degradation of toxic dyes under visible irradiation*. Composites Part B: Engineering, 2019, **175**: 107080.
16. Poorbafrani, A., and E. Kiani, *Enhanced microwave absorption properties in cobalt–zinc ferrite based nanocomposites*. Journal of Magnetism and Magnetic Materials, 2016, **416**: p. 10-14.
17. Qin, M., et al. *Zinc ferrite composite material with controllable morphology and its applications*. Materials Science & Engineering B, 2017, **224**: p. 125-138.
18. Annie Vinosha, et al., *Synthesis and properties of spinel $ZnFe_2O_4$ nanoparticles by facile co-precipitation route*. Optik, 2017, **134**: 99-108.
19. Yadav, R. S., et al., *Structural, magnetic, optical, dielectric, electrical and modulus spectroscopic characteristics of $ZnFe_2O_4$ spinel ferrite nanoparticles synthesized via honey-mediated sol-gel combustion method*. Journal of Physics and Chemistry of Solids. 2017, **110**: p. 87-99.
20. Hajian Karahroudi, Z., et al., *Green synthesis and characterization of hexaferrite strontium-perovskite strontium photocatalyst nanocomposites*. Main group metal chemistry, 2020, **43**: p. 26-42.
21. Rachna, et al., *Sunlight mediated improved photocatalytic degradation of carcinogenic benz[a] anthracene and benzo[a]pyrene by zinc oxide encapsulated hexacyanoferrate nanocomposite*. Journal of Photochemistry and Photobiology A: Chemistry, 2019, **381**: 111861.
22. Farooq, A., et al., *Cellulose from sources to nanocellulose and an overview of synthesis and properties of nanocellulose/zinc oxide*. International Journal of Biological Macromolecules, 2020, **154**: p. 1050-1073.
23. Kuang, M., et al., *Synthesis of octahedral-like ZnO/ZnFe2O4 heterojunction photocatalysts with superior photocatalytic activity*. Solid State Sciences, 2019,**96**:105901.
24. Hedayati, K., et al., *Magnetic and Photo-catalyst $CoFe_2O_4$-CdS nanocomposites: Simple preparation of Ni, Co, Zn or Ag-doped CdS nanoparticles*. Journal of Materials Science: Materials in Electronics, 2017, **28**: p. 5472-5484.
25. Zamiri, R., et al., *Optical and magnetic properties of ZnO/$ZnFe_2O_4$ nanocomposite*. Materials Chemistry and Physics, 2017, **192**: p. 330–338.